taken as unequivocal evidence for internal mobility on the nanosecond time scale. We note, however, the ^2H quadrupolar relaxation would yield information on motions whose correlation times $\tau \leq \tau_m$. Hence, ^2H NMR in the liquid state is incapable of characterizing a range of motions slower than τ_m that would be consistent with the intuitive pictures of flexibility implied by other data.[5,6]

Conclusion

We demonstrated that ^2H signals from individual sites in a paramagnetic protein can be detected, resolved, and characterized. The peaks located in the diamagnetic envelope are consistent with assignments obtained by indirect methods.[44,45] The ^2H NMR line widths were shown to be predominantly quadrupolar in origin, even for highly paramagnetic systems, and allow direct interpretation of this data in terms of mobility. Skeletal labels reveal an immobile prosthetic group within the heme cavity. Methyl groups reflected rapid internal rotation. The vinyl ^2H labels did not exhibit sufficient narrowing to be unequivocally interpreted in terms of internal mobility. It is suggested that heme methyl ^2H line widths afford a valuable probe for the determination of protein tumbling times in paramagnetic heme protein derivatives.

(49) Determination of the vinyl ^2H quadrupolar coupling constant, even in the solid state, may be rendered ambiguous if internal motion persists.

Acknowledgment. Useful discussions with J. T. J. Lecomte and Professor R. R. Vold and the experimental assistance of G. B. Matson are gratefully acknowledged. The research was supported by grants from the National Science Foundation (CHE-81-08766, CHE-84-15329) and the National Institutes of Health (HL-22252).

Proton Nuclear Magnetic Resonance Investigation of the Mechanism of the Reconstitution of Myoglobin That Leads to Metastable Heme Orientational Disorder

Gerd N. La Mar,* Usha Pande, Jon B. Hauksson, Ravindra K. Pandey, and Kevin M. Smith

Contribution from the Department of Chemistry, University of California, Davis, California 95616. *Received March 24, 1988*

Abstract: The nature of the initially formed complexes between sperm whale apomyoglobin and hemin has been investigated by ^1H NMR for the purpose of elucidating the factors that give rise to heme orientational disorder in the reconstitution process. Selective removal of each of the two propionate side chains leads to an initial complex upon reconstitution (in the presence of a non-interacting organic solvent) with strong selectivity for the heme orientation which places the sole propionate into the position occupied by the 6-propionate group in the crystal structure. Hence the propionate contacts with apomyoglobin lead to the heme disorder about the α,γ-meso axis. Equilibration yields a unique heme orientation identical to that found in native Mb single crystals. Reconstitution of apomyoglobin with iron-free protoporphyrin yields only a single heme orientation within the time needed to obtain a NMR spectrum. However, this is concluded to result from rapid equilibration rather than from unique insertion of the porphyrin. The larger ring current for the des-iron myoglobin complex is interpreted in terms of protonation of the His F8 side chain that interacts with the porphyrin core. Pyridine is shown to interact strongly with cyanomet myoglobin, and the induced changes in hyperfine shifts show a spatial selectivity which suggests that pyridine intercalates on the proximal side of the heme.

The reactions between apomyoglobin (apoMb) or apohemoglobin (apoHb) and hemin initially were thought to be complete within seconds to yield the native holoprotein on the basis of optical stopped-flow studies.[1,2] More recently, however, ^1H NMR investigations have demonstrated[3-8] that these reactions instead yield as initial products the 1:1 mixtures of holoproteins with the orientations of the heme in the folded pocket differing by a 180° rotation about the α,γ-meso axis, as shown in A and B of Figure 1 (with $R_6 = R_7$ = propionate). Only one of these orientations corresponds to that found in single crystals[9,10] (Figure 1A). The "reversed" heme orientation (Figure 1B) is kinetically trapped, and this requires many hours to months to equilibrate to the native protein, depending upon the protein origin and the solution conditions.[3,5,6,8] Moreover, this "reversed" heme orientation does not disappear, but it is present to some extent at equilibrium in both Mbs and Hbs, as clearly observed in the ^1H NMR spectra of isolated native proteins.[5-7] ^1H NMR spectroscopy is uniquely and ideally suited for both detecting and quantitatively characterizing this heterogeneity in hemoproteins.[3-8] Qualitative characterization of changes in the ratio of heme orientation can now also be monitored by circular dichroism.[11-14]

* Address correspondence to this author.

(1) Gibson, Q. H.; Antonini, E. *Biochem. J.* **1960**, *77*, 328-341.
(2) Gibson, Q. H.; Antonini, E. *J. Biol. Chem.* **1962**, *238*, 1384-1388.
(3) Jue, T.; Krishnamoorthi, R.; La Mar, G. N. *J. Am. Chem. Soc.* **1983**, *105*, 5701-5703.
(4) La Mar, G. N.; Davis, N. L.; Parish, D. W.; Smith, K. M. *J. Mol. Biol.* **1983**, *168*, 887-896.
(5) La Mar, G. N.; Toi, H.; Krishnamoorthi, R. *J. Am. Chem. Soc.* **1984**, *106*, 6395-6401.
(6) Levy, M. J.; La Mar, G. N.; Jue, T.; Smith, K. M.; Pandey, R. K.; Smith, W. S.; Livingston, D. J.; Brown, D. W. *J. Biol. Chem.* **1985**, *260*, 13694-13698.
(7) La Mar, G. N.; Yamamoto, Y.; Jue, T.; Smith, K. M.; Pandey, R. *Biochemistry* **1985**, *24*, 3826-3831.
(8) Yamamoto, Y.; La Mar, G.N. *Biochemistry* **1986**, *25*, 5288-5297.
(9) Takano, T. *J. Mol. Biol.* **1977**, *110*, 537-568.
(10) Baldwin, J. M. *J. Mol. Biol.* **1980**, *136*, 103-128.
(11) Aojula, H. S.; Wilson, T. M.; Drake, A. *Biochem. J.* **1986**, *237*, 613-616.
(12) Light, W. R.; Rohlfs, R. J.; Palmer, G.; Olson, J. S. *J. Biol. Chem.* **1987**, *262*, 46-52.
(13) Belleli, A.; Foon, R.; Ascoli, F.; Brunori, M. *Biochem. J.* **1987**, *246*, 787-789.

0002-7863/89/1511-0485$01.50/0

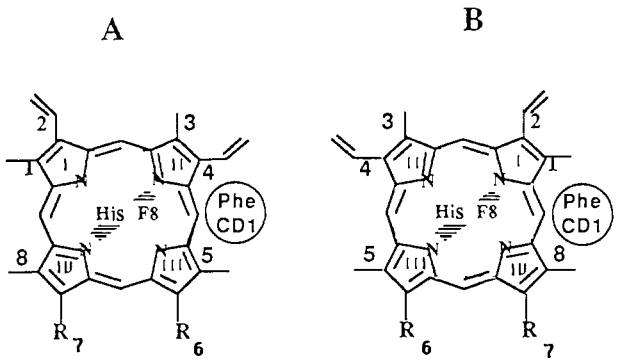

Figure 1. The two alternate orientations of hemin (R_6 = R_7 = propionate) in the folded pocket of sperm whale Mb. Orientation A corresponds to the orientation found in single crystals,[9] and B is rotated by 180° about the α,γ-meso axis.[4] In both 6-methyl-6-despropionate-hemin (R_6 = methyl, R_7 = propionate) and 7-methyl-7-despropionate-hemin (R_6 = propionate, R_7 = methyl) reconstituted into sperm whale Mb, the orientation as in A has been found[21] strongly dominant at equilibrium.

The relative stabilities of the two heme orientations depend on the nature of the polypeptide chain, the oxidation/ligation state of the iron, and the substituents on the porphyrin.[3-8,15-17]

Little is known about the mechanism of the initial interaction between hemin and apoprotein which yields this isomeric incorporation of the heme into the heme pocket. To date, some 15 hemes possessing a permutation of substituents at the 2- and/or 4-positions and propionates at positions 6 and 7 have all yielded[4,6,8,15,16] the same pair of isomers (A and B in Figure 1) during the initial reaction with sperm whale apoMb, and in all but one case the equilibrated protein exhibits one dominant orientation that is the same as that found for hemin in the native protein single crystals.[9,10,16] Kinetic studies of the heme equilibration in sperm whale Mb have been carried out on met-aquo and met-cyano forms,[3,5,11,12] where the reaction was found to have both acid- and base-catalyzed steps, with the rate constants ~10 larger for the high-spin than the low-spin species.

We are interested in this report in ascertaining aspects of the reconstitution mechanism which give rise to the initially formed heterogeneous holoprotein. Specifically, what are the features of the initial interaction between the hemin and apoprotein that lead to the alternate modes of heme insertion? The nature of the two initially formed isomeric Mb complexes (A and B in Figure 1) suggests one of two likely mechanisms for their formation. On the one hand, the initial interaction could involve formation of the iron–imidazole bond to His F8, followed by relaxation of the heme pocket to form the holoprotein at a rate rapid compared to the axial bond lability. By the time the relaxed pocket senses the non-equivalence of the two sides of the heme at pyrroles I and II, the heme is kinetically trapped in the metastable orientation in half of the molecules. Since the apoprotein possesses[18] less tertiary structure than the holoprotein, the initial encounter is not likely to differentiate between the two sides of the heme plane which, upon rotation about the axial bond to match hydrophobic and hydrophilic environments in the heme pocket, could lead to the two forms depicted in A and B of Figure 1.

An alternate mechanism could have the important initial interaction between the hemin and apoprotein involving the formation of one (or both) of the salt bridges between the heme propionates and the partner contacts in the heme pocket,[9] Arg CD3 and/or His FG3, followed by the rapid formation of the axial bond and the relaxation of the heme pocket to that of the holoprotein. The presence of two propionates symmetrically placed with respect to the α,γ-meso axis of hemin would lead to the two observed isomeric incorporations[4,5] of the heme (A and B in Figure 1). The two mechanisms, at least in principle, can be differentiated by monitoring the initially formed species upon reconstitution when either the iron–His bond or one of the propionate salt bridges is not able to form because of modification of the prosthetic group.

The iron–His F8 bond can be abolished by reacting apoMb with iron-free hemin or protoporphyrin IX (Figure 1, with R_6 and R_7 = propionate and removal of iron). The free porphyrin reconstitutes to yield a metal-free Mb with tertiary structure very similar to that of the holoprotein.[19] The role of the propionates can be addressed by selectively replacing each of the two propionates with a methyl. Such hemin derivatives have been synthesized.[20] Structural studies[21] on equilibrated sperm whale Mb reconstituted with hemins having either the 6- or 7-propionate replaced by a methyl group (6-methyl-6-despropionate-hemin (Figure 1, R_6 = CH_3, R_7 = propionate), and 7-methyl-7-despropionate-hemin (Figure 1, R_6 = propionate, R_7 = CH_3)) have yielded equilibrium heme orientations that are the same as for native hemin[9] for both derivatives. Thus the equilibrium heme orientation was found to be completely determined by the hydrophobic interaction between the protein and pyrroles I and II of the heme. The need to use mixed solvent systems to dissolve these hemes[21] and the time necessary to remove these solvents yielded proteins that had reached equilibrium by the time ^1H NMR measurements were made. By rapid removal of the organic component by gel filtration, we are able here to detect the metastable species formed immediately after reconstitution.

Experimental Section

Reconstitution of Mb. Sperm whale Mb was obtained from Sigma Co. and used without further purification. ApoMb was prepared according to reported procedures.[5,22] Solutions ~1.5 mM in apoMb in ^2H_2O were buffered with phosphate (100 mM, pH 5.7–5.8), any precipitate removed by centrifugation, and the final concentration of apoMb determined by optical intensity (ϵ = 15 900 M^{-1} cm^{-1} at 280 nm).

Native hemin (Figure 1, R_6 = R_7 = propionate) was obtained from Man-Win Chemicals, and 7-(2-carboxyethyl)-1,3,5,6,8-pentamethyl-2,4-divinylhemin (hereafter referred to as 6-methyl-6-despropionate-hemin; Figure 1 with R_6 = CH_3, R_7 = propionate) and 6-(2-carboxyethyl)-1,3,5,7,8-pentamethyl-2,4-divinylhemin (hereafter referred to as 7-methyl-7-despropionate-hemin; Figure 1 with R_6 = propionate, R_7 = CH_3) were prepared as described previously.[20] The stoichiometric amounts of hemins were dissolved in the presence of a 6-fold excess of cyanide in a mixed solvent of ^2H_2O and either pyridine or dimethyl sulfoxide, DMSO, to yield a final protein solution 5% by volume of organic co-solvent. The organic component is necessary to dissolve the modified hemins.[21] The pH of the solution was immediately adjusted to 7.0 with 0.1 M ^2HCl. The solvent was exchanged with ^2H_2O containing 0.2 M NaCl, pH 7.0, using either an Amicon ultrafiltration cell or gel-filtration[23] with a 20-cm column of Sephadex G25. Protoporphyrin IX (Figure 1 with R_6 = R_7 = propionate and the iron removed) was obtained from hemin by removal of the iron. It was dissolved in 0.1 M NaO^2H in ^2H_2O and added dropwise to the buffered apoMb. NMR measurements were initiated within 10 min of reconstitution.

The sample pH was measured with a Beckman 3550 pH meter equipped with an Ingold micro-combination electrode; the reported pH values are not corrected for the isotope effect.

^1H NMR Measurements. ^1H NMR spectra were recorded at 25 °C on Nicolet/GE NT-360 and NT-500 FT NMR spectrometers operating in quadrature at 360 and 500 MHz, respectively. The met-cyano complexes required ~2×10^3 transients collected over a 12 kHz bandwidth, with a pulse repetition rate of 1 s^{-1}, and the met-pyridine complex needed 5×10^3 transients over 40 kHz with a pulse repetition rate of 10 s^{-1}. The diamagnetic des-iron Mb ^1H NMR spectrum was collected over an 8 kHz bandwidth requiring 500 transients at a pulse repetition rate of 0.5 s^{-1}. The residual water signal was suppressed by a low-power decoupler pulse.

(14) Kawamura-Konishi, Y.; Kihara, H.; Suzuki, H. *Eur. J. Biochem.* **1988**, *170*, 589–595.
(15) Davis, N. L. Ph.D. Dissertation, University of California, Davis, 1983.
(16) Mibi, K.; Ii, Y.; Yukawa, M.; Owatari, A.; Hato, Y.; Harada, S.; Kai, Y.; Kasai, N.; Hata, Y.; Tanaka, N.; Kakudo, M.; Katsubi, Y.; Yoshida, Z.; Ogoshi, H. *J. Biochem.* **1986**, *100*, 209–276.
(17) La Mar, G. N.; Budd, D. L.; Viscio, D. B.; Smith, K. M.; Langry, K. C. *Proc. Natl. Acad. Sci. U.S.A.* **1978**, *75*, 5755–5759.
(18) Breslow, E.; Beychok, S.; Hardman, K. D.; Gurd, F. R. N. *J. Biol. Chem.* **1965**, *240*, 304–309.
(19) Jameson, D. M.; Gratton, E.; Weber, G.; Alpert, B. *Biophys. J.* **1984**, *45*, 739–803.
(20) Smith, K. M.; Craig, G. W. *J. Org. Chem.* **1983**, *48*, 4302–4306.
(21) La Mar, G. N.; Emerson, S. D.; Lecomte, J. T. J.; Pande, U.; Smith, K. M.; Craig, G. W.; Kehres, L. A. *J. Am. Chem. Soc.* **1986**, *108*, 5568–5573.
(22) Teale, F. W. J. *Biochim. Biophys. Acta* **1959**, *35*, 543.
(23) Johnston, P. D.; Figueroa, N.; Redfield, A. G. *Proc. Natl. Acad. Sci. U.S.A.* **1979**, *76*, 3130–3134.

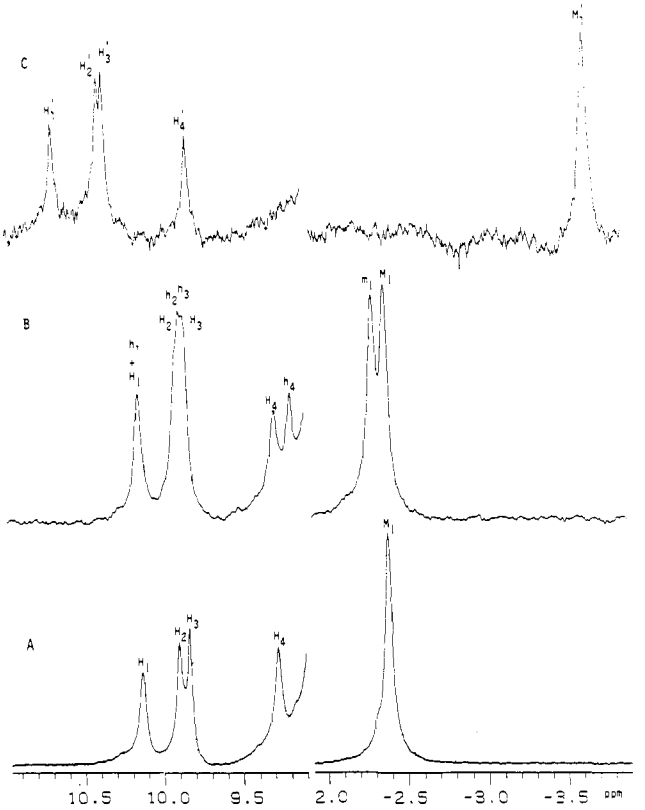

Figure 2. The resolved portions of 500-MHz ^1H NMR spectra of diamagnetic sperm whale Mb complexes in ^2H_2O, 25 °C and pH 7.0, illustrating the low-field region where the four meso-H resonate, and the upfield ring current-shifted region where the Val E11 γ-CH_3 is resolved.[24] A, native MbCO; B, freshly reconstituted MbCO which exhibits doubling of peaks due to the heme disorder described in Figure 1; C, the complex of protoporphyrin IX and sperm whale apoMb,[19] desFe Mb, taken within 24 min after reconstitution; note only a single set of four meso-H peaks and a single upfield peak. The spectrum exhibited no change with time over several weeks.

Table I. Chemical Shifts of Meso-H and Val E11 γ-CH_3 Peaks in Diamagnetic Mb Complexes[a]

	MbCO				desFe Mb	
	isomer A[b]		isomer B[b]		isomer A[b]	
meso-H	H_1	10.10	h_1	10.10	H_1'	10.70
meso-H	H_2	9.90	h_2	9.87	H_2'	10.40
meso-H	H_3	9.80	h_3	9.82	H_3'	10.30
meso-H	H_4	9.30	h_4	9.15	H_4'	9.80
Val E11 γ_2-CH_3	M_1	−2.39	m_1	−2.28	M_1'	−3.68

[a] Shifts in ppm from DSS in ^2H_2O, pH 7.0. [b] Isomer A and B refers to heme orientation as in Figure 1, parts A and B, respectively (with R_6 = R_7 = propionate).

Chemical shifts are in ppm from internal 2,2-dimethyl-2-pentane-5-sulfonate, DSS.

Results

Reaction of apoMb with Protoporphyrin. The resolved portions of the 500-MHz ^1H NMR spectrum of diamagnetic native MbCO are illustrated in spectrum A of Figure 2 and display the four low-field meso-H peaks, H_1–H_4, and the resolved upfield Val E11 γ_2-CH_3 peak,[24] M_1. The similar protons of the NMR trace of a freshly reconstituted MbCO complex are shown in spectrum B of Figure 2. In addition to the clear doubling of the upfield γ_2-CH_3 peak, previously shown to reflect the 1:1 heme orientational disorder,[3] we note that the meso-H peaks also exhibit the heterogeneity. Thus, one of the reversed heme orientation peaks is completely resolved (h_4), two are partially resolved (h_2, h_3), and one (h_1) is degenerate with peak H_1. The chemical shifts are listed in Table I.

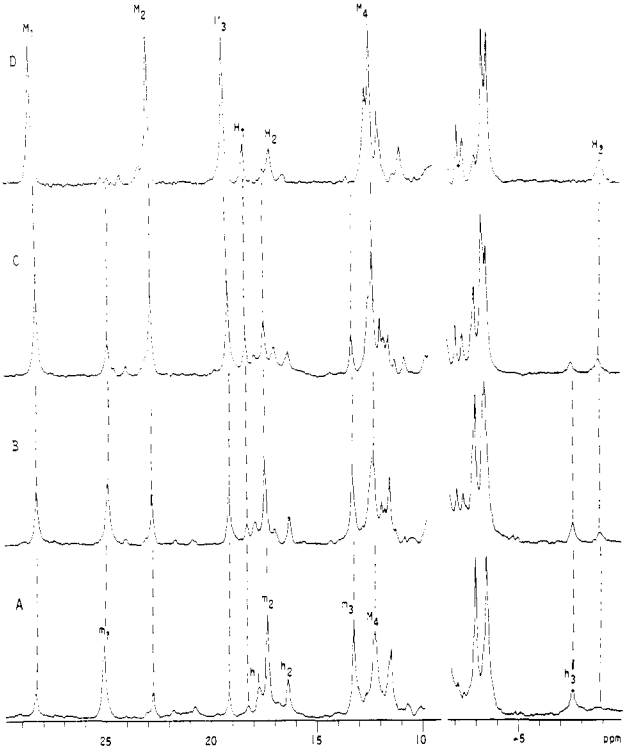

Figure 3. The resolved hyperfine-shifted portions of the 360-MHz ^1H NMR spectra (25 °C, pH 7.0) of sperm whale apoMb reconstituted with 6-methyl-6-despropionate-hemin (R_6 = CH_3, R_7 = propionate in Figure 1) in (A) 5% DMSO/95% ^2H_2O in the presence of excess CN^-, with the DMSO immediately removed by gel filtration, and in (B) 5% pyridine/95% ^2H_2O in the presence of excess CN^-, with the pyridine immediately removed by gel filtration. Spectra C and D are the traces of the same sample as in B, after 2300 min and at equilibrium, respectively. The assignments of the dominant isomer at equilibrium are M_i and H_i for methyls and single protons, while the peaks for the initial isomer are similarly designated m_i, h_i. The resonance M_1, H_i have been previously assigned by NOEs.[21]

The resolved portions of the 500-MHz ^1H NMR spectrum of the freshly formed complex between protoporphyrin IX[19] (iron-free hemin, R_6 = R_7 = propionate, Figure 1) and apoMb are shown in Figure 2C. The low-field portion reveals the characteristic four single-proton meso-H peaks at 10.7, 10.4, 10.3, and 9.8 ppm, while the upfield region yields only a methyl peak that can be assigned to γ_2-CH_3 of Val E11 due to the porphyrin ring current.[24] Deconvolution does not lead to any evidence of splitting of any of the resolved peaks, and the spectrum exhibits no changes in peak positions or line widths as a function of time up to several weeks (not shown). Thus the ^1H NMR spectrum initially recorded (within 24 min of reconstitution) reflects that of the protein complex at equilibrium and exhibits peaks consistent with only a single species. The chemical shifts are included in Table I.

Reaction of apoMb with 6-Methyl-6-despropionate-Hemin. The ^1H NMR trace of the initial met-cyano complex formed upon reacting apoMb with 6-methyl-6-despropionate-hemin in 5% DMSO-$^2H_6$:95% ^2H_2O solution containing excess CN^- (and the DMSO removed by gel filtration)[23] is illustrated in spectrum A of Figure 3. The trace contains the heme methyl peaks, M_1 (5-CH_3), M_2 (6-CH_3), M_3 (1-CH_3), M_4 (8-CH_3), and single proton peak H_3 (Ile 99 γ-CH), earlier identified[21] with the equilibrium heme orientation (A in Figure 1, R_6 = CH_3, R_7 = propionate), but this species is a minor component relative to that which yields the apparent heme methyl peaks m_1, m_2, and m_3 and Ile 99 peak, h_3. The relative abundance of the two species which give rise to the set of peaks m_i, h_i and M_i, H_i is ~3.8. If the reaction between apoMb is carried out with this modified hemin in a 5% pyridine-$^2H_5$:95% ^2H_2O solution containing excess CN^- (with pyridine subsequently removed by rapid gel filtration), the

(24) Mabbutt, B. C.; Wright, P. E. *Biochim. Biophys. Acta* **1985**, *832*, 175–185.

Table II. Chemical Shifts of metMbCN Reconstructed with Modified Hemins[a]

	6-methyl-6-despropionate-hemin-metMbCN			
	isomer A[b]		isomer B[b]	
heme methyl	M_1(5-CH_3)[c]	28.1	m_1(8-CH_3 ?)[f]	24.7
heme methyl	M_2(6-CH_3)[c]	22.6	m_2(3-CH_3 ?)[f]	17.3
heme methyl	M_3(1-CH_3)[c]	19.0	m_3(5-CH_3 ?)[f]	13.2
heme methyl	M_4(8-CH_3)[c]	12.1		
vinyl Hα[d]	H_1	16.8	h_2	16.1
Phe CD1 pH[e]	H_2	15.5	h_1	17.8
Ile FG5 γ-CH[e]	H_3	−9.0	h_3	−7.7
	7-methyl-7-despropionate-hemin-metMbCN			
	isomer A[b]		isomer B[b]	
heme methyl	M_1(5-CH_3)[c]	24.9	m_1(8-CH_3 ?)[f]	28.6
heme methyl	M_2(1-CH_3)[c]	17.8	m_2(7-CH_3 ?)[f]	21.4
heme methyl	M_3(8-CH_3)[c]	13.1	m_3(3-CH_3 ?)[f]	18.1
heme methyl			m_4(5-CH_3 ?)[f]	12.1
vinyl H$_\alpha$[d]	H_1	17.3	*g*	
Phe CD1 pH[e]	H_2	17.3	*g*	
Ile FG5 γ-CH[f]	H_3	−8.6	*g*	

[a] Shifts in ppm from DSS in ^2H_2O, pH 8.6. [b] Isomer A and B refers to heme orientations as in Figure 1, parts A and B, respectively. [c] Assignments reported based on NOEs. [d] Reference 21. [e] Reference 25. [f] Tentative assignment based on predictions of shifts for the orientation, as given in ref 21. [g] Too weak to be detected clearly.

initial spectrum observed is that shown in spectrum B of Figure 3. The same two sets of peaks M_i, H_i and m_i, h_i are present as when DMSO was used, except that the intensity of the set corresponding to the intermediate, m_i, h_i, to that of the equilibrium heme orientation, M_i, H_i, is only ~1.5. With either co-solvent (data shown for the case when reconstitution took place with pyridine), the set of peaks M_i, H_i gains intensity with time (spectrum C of Figure 3) at the expense of that set m_i, h_i. At equilibrium, the set M_i, H_i dominates over the set m_i, h_i by a ratio of ~20 and corresponds to the heme orientation shown in A of Figure 1, as determined previously from NOE data.[21] The shifts of the two sets of resonances are listed in Table II.

Reaction of apoMb with 7-Methyl-7-despropionate-Hemin. The resolved hyperfine shifted portions of the 360-MHz ^1H NMR spectrum of 7-methyl-7-despropionate-hemin (Figure 1, R_6 = propionate, R_7 = CH_3) immediately after reconstitution in a 5% DMSO/95% ^2H_2O solution are illustrated in spectrum A of Figure 4; the DMSO has been removed by rapid gel filtration. The obvious heme methyl peaks previously unambiguously assigned[21] by NOEs are labeled M_1 (5-CH_3), M_2 (1-CH_3), and M_3 (8-CH_3); the prominent Ile FG5 γ-H peak (H_3) is located upfield. This spectrum is essentially identical with that observed for the completely equilibrated protein,[21] and hence predominantly a single species is formed in the initial complex which is also the most stable species.

When the same reaction is carried out between apoMb and 7-methyl-7-despropionate-hemin in 5% pyridine:95% ^2H_2O solution containing excess CN^-, the initial ^1H NMR spectrum observed upon rapid removal of the pyridine is that shown in spectrum B of Figure 4. While the dominant peaks are the same ones (M_1, M_2, M_3, H_1, H_2, H_3) observed when DMSO was used as co-solvent, a second set of peaks is now detected for which m_1, m_2, m_3, and m_4 have areas for methyl protons and h_3 consists of a single proton. The second set of peaks, m_i, h_i, loses intensity with time, while the set M_i, H_i gains intensity until equilibrium is reached (trace D, Figure 4). The final ratio of intensity of M_i/m_i is ~18. The shifts for the two sets of peaks are included in Table II.

Interaction of Organic Solvents with Mb. When ^1H NMR spectra were observed initially after reconstitution in the presence of the organic component, the shifts, line widths, and relative intensities varied insignificantly due to the presence of DMSO, but a very substantial influence in both shifts and line widths (though *not* relative intensity) was observed due to the presence of pyridine-$^2H_5$. The nature of the apparent interaction of Mb with puridine-$^2H_5$ was explored in detail only with native Mb and the protein initially reconstituted with native hemin (Figure 1, R_6 = R_7 = propionate).

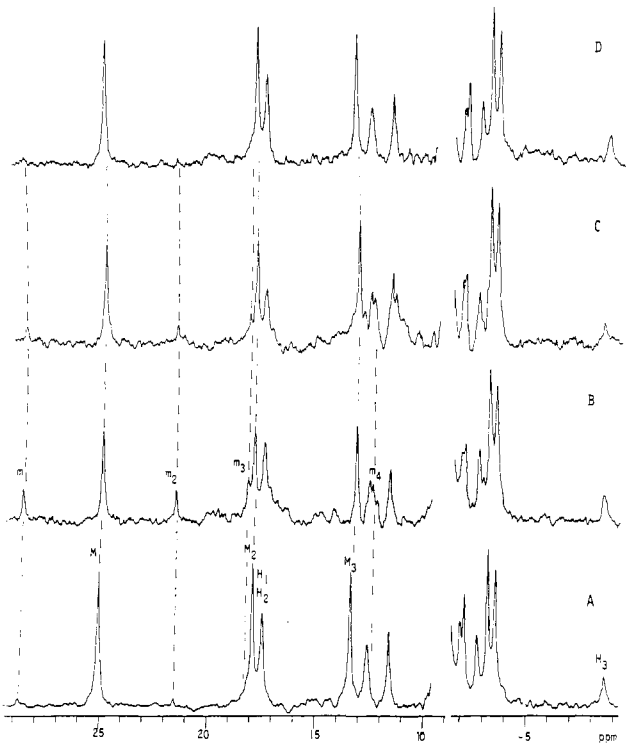

Figure 4. The resolved hyperfine-shifted portions of the 360-MHz ^1H NMR spectra (25 °C, pH 7.0) of sperm whale apoMb reconstituted with 7-methyl-7-despropionate-hemin (R_6 = propionate, R_7 = CH_3 in Figure 1) in (A) 5% DMSO/95% ^2H_2O in the presence of excess CN^-, with the immediate removal of DMSO by gel filtration, and in (B) 5% pyridine/95% ^2H_2O in the presence of excess CN^-, with the immediate removal of pyridine by gel filtraton. Spectra C and D are the traces of the same sample in B after 2200 min and at equilibrium, respectively. The assignments are M_i, H_i for the major and m_i, h_i for the minor component methyls and single protons, respectively. The peaks M_i, H_i have been previously assigned by NOEs.[21]

The trace of native metMbCN in ^2H_2O is reproduced in spectrum A of Figure 5 and can be compared to that of the same native complex in 5% pyridine-$^2H_5$ (Figure 5C), which obviously experiences significant changes in shifts and line widths for numerous resonances. In contrast, the ^1H NMR trace for metMbCN in 5% DMSO-$^2H_5$ (Figure 5B) is essentially indistinguishable from that in pure ^2H_2O (trace A). The effect on resonance position and line width upon titrating pyridine-$^2H_5$ to a metMbCN solution in pure ^2H_2O leads to a single set of resonances under all conditions, with the shifts varying monotonically with the amount of added pyridine-$^2H_5$. A plot of the chemical shift as a function of pyridine-$^2H_5$ increment (in mole percent) for the resolved and assigned resonances shown in spectrum A of Figure 5 is given in Figure 6. The shifts reach asymptotic values at large (~2 mol %) pyridine concentration. Analysis of the curves based on the existence of a simple equilibrium involving a complex with a single pyridine-$^2H_5$ molecule interacting with Mb yields a binding constant of ~3.8 M^{-1}. The incremental effects of saturating amounts of pyridine-$^2H_5$ on chemical shifts of assigned resonances of metMbCN are listed in Table III.

Comparison of the ^1H NMR trace of metMbCN in the presence of 5% pyridine-$^2H_5$ (Figure 5B) with that of metMbH_2O in the presence of 5% pyridine-$^2H_5$ (i.e., no cyanide present; Figure 5D) clearly shows that different species result. Lastly, if the reconstitution of apoMb with native hemin is carried out in the presence of excess cyanide and 5% pyridine-$^2H_5$, two sets of signals appear with identical intensities (Figure 5E), one of which is the same as that observed for native metMbCN in the presence of pyridine-$^2H_5$ (Figure 5C). When the pyridine-$^2H_5$ is removed from the sample used to obtain trace 5E, the two sets of resonances with identical intensities that are associated with the two orien-

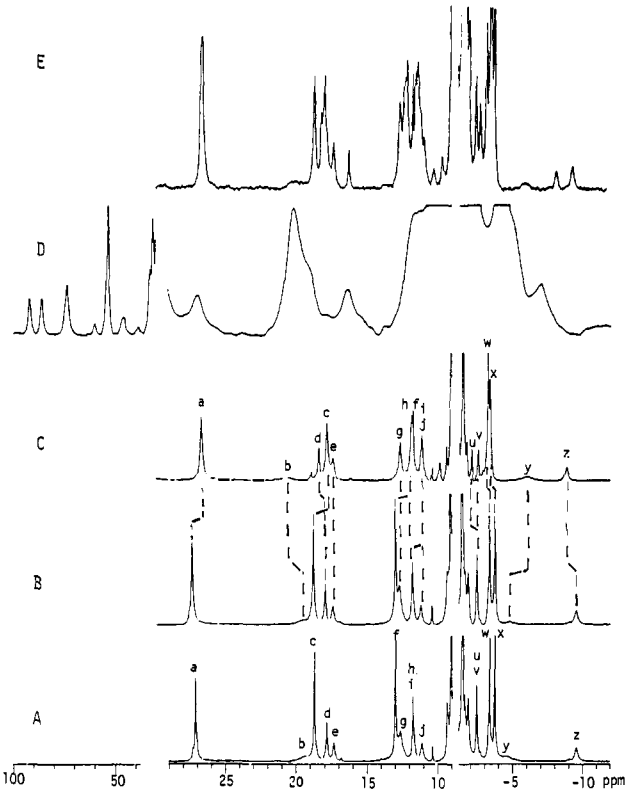

Figure 5. Resolved portions of the hyperfine-shifted 360-MHz ^1H NMR spectra of (A) native metMbCN in ^2H_2O, (B) native metMbCN in5% DMSO-$^2H_6$/95% ^2H_2O, and (C) native metMbCN in 5% pyridine-$^2H_5$/95% ^2H_2O; note the very strong similarity of traces in A and B and the strong influence on shifts (indicated by dotted lines) in trace C. Spectrum D show the NMR trace of metMbH_2O in 5% pyridine-$^2H_5$/95% H_2O (in the absence of CN^-) which is completely different from that in trace C; note the horizontal compression of the trace in the region 50–100 ppm. Trace E shows the NMR spectra of apoMb freshly reconstituted with native hemin in 5% pyridine $^2H_5$/95% ^2H_2O; note the doubling of lines, in particular a and z, indicating that the two orientations are formed equally in the presence of pyridine.

tations of the native hemin, as reported in detail previously,[4,5] appear (not shown).

Table III. Chemical Shifts for Native Sperm Whale Met-Myoglobin Cyanide and Its Complexes with Pyridine

peak	assignment	chemical shift[a]	shift change[b]
a	5-CH_3[c]	27.13	−0.64
b	His F8 ring CH[d]	19.40	+1.20
c	1-CH_3[c]	18.63	−1.13
d	2-vinyl H_α[e]	17.74	+0.66
e	Phe CD1 p-H[f]	17.27	−0.03
f	8-CH_3[c]	12.90	−1.56
g	Phe CD1 m-Hs[f]	12.55	−0.03
h	His E7 $C_\beta H$[g]	11.67	−0.07
i	His F8 $C_\beta H$[g]	11.67	−0.79
u	2-vinyl-$H_{\beta t}$[e]	−2.61	+0.51
v	Val E11 $C_\alpha H$[h]	−2.61	−0.12
w	Ile FG5 γ-CH_3[i]	−3.53	+0.21
x	Ile FG5 δ-CH_3[i]	−3.90	+0.49
y	His F8 ring CH[d]	−4.66	−1.78
z	Ile FG5 CγH[i]	−9.73	+1.06

[a] Shift in ppm from DSS at 25 °C, pH 8.0 for metMbCN in ^2H_2O. [b] Change in chemical shift upon adding 2 mol% pyridine-$^2H_5$, which corresponds to formation of the pyridine intercalation complex; positive (negative) changes are downfield (upfield). [c] References 4 and 28. [d] Reference 27. [e] Reference 29. [f] Reference 25. [g] Reference 30. [h] Reference 31. [i] Reference 32.

Discussion

Mechanism of Reconstitution. The sizable shift difference for both meso-H and Val E11 γ-CH_3 peaks between the two heme orientations in MbCO (Figure 2A,B) clearly demonstrates that this heterogeneity is resolved in a diamagnetic complex.[3] The reaction of apoMb and protoporphyrin (iron-free hemin) yields only a single detectable species in the minimal time (~20 min) needed to collect ^1H NMR data after reconstitution, and the nature of this species does not change with time. Hence, either formation of the iron–His bond is the critical step in the initial encounter that causes metastable heme disorder or else both protoporphyrin orientations are formed initially, but the rate of reorientation is so fast that equilibrium is reached by the time ^1H NMR data can be collected. Thus these measurements are inconclusive with respect to differentiating between the two proposed alternative cases.

The influence of removing propionate contacts is more illuminating. Reconstitution of 6-methyl-6-despropionate-hemin in

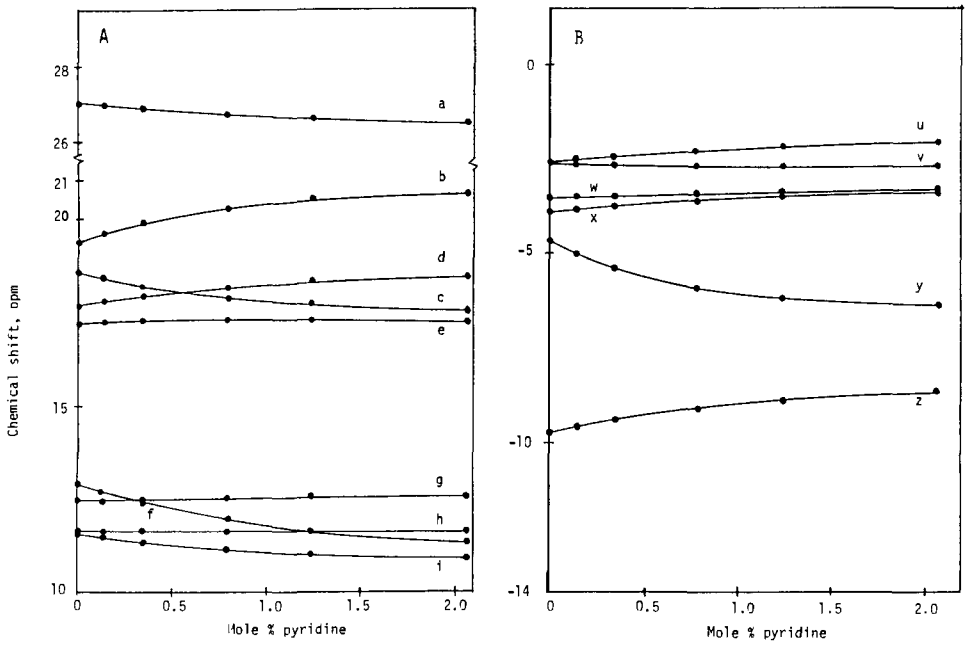

Figure 6. Plots of the chemical shifts, in ppm from DSS at 25 °C, for low-field (A) and high-field (B) resolved and assigned signals of metMbCN in ^2H_2O as a function of increasing amounts of pyridine-$^2H_5$ (in mol %). The lines represent fits to a 1:1 equilibrium constant between metMbCN and pyridine-$^2H_5$, with $K \sim 3.8$ m^{-1}. The increment shifts upon forming the 1:1 complexes are given in Table III.

the presence of either DMSO-$^2H_5$ or pyridine-$^2H_5$ leads to a strong preference (much more so for DMSO than pyridine) for an *initial product different from the equilibrated product*. The methyl shifts for the initial product (m_1, m_2, m_3) have precisely the shifts predicted[21] for that hemin rotated by 180° about the α,γ-meso axis, i.e. with orientation as in B of Figure 1. This allows the tentative assignments m_1 = 8-CH_3, m_2 = 3-CH_3, m_3 = 5-CH_3, and h_1 = p-H of Phe CD1[25] and h_3 = γ-CH of Ile FG5 (Table II).

In the case of reconstitution of 7-methyl-7-despropionate-hemin (Figure 4), the initial product heavily favors the species that is identical to the equilibrated product, whose orientation has been established[21] as in A of Figure 1. However, a small amount of a second species is formed (very noticeable in pyridine-$^2H_5$), with four apparent methyl peaks with shifts as predicted for the hemin orientation as in B of Figure 1, i.e. rotated by 180° about the α,γ-meso axis. This allows the tentative assignment[21] of the alternate orientation, m_1 = 8-CH_3, m_2 = 7-CH_3, m_3 = 3-CH_3, m_4 = 5-CH_3; the single proton peaks h_i are too weak to detect clearly.

The removal of individual propionate side chains thus clearly indicates strong preferences for the orientation of the hemin in the initially formed encounter complex, with the preferred orientation in each case having the single propionate in the position that makes the protein link characteristic of the 6-propionate in the native holoprotein.[9] This link in the native protein[9] is with the surface residue Arg CD3. Thus the preference for the initial orientation supports the importance of the formation of a salt bridge between the apo-protein and *only one of the two heme propionates* in determining metastable heme orientational disorder and that this link likely involves Arg CD3 on the protein surface.

Dynamics of Heme Reorientation. The rate of intensity loss of the sets of methyl peak m_i in both 6-methyl-6-despropionate-hemin (Figure 3) and 7-methyl-7-despropionate-hemin (Figure 4) reflects a half-life ~30–40 h at pH ~8 and 25 °C, which is very similar to that also observed for the reorientation of native hemin in the met-cyano complex.[3,5] Thus the breaking of the salt bridges involving the propionates does not appear to be rate controlling in the mechanism of heme reorientation which likely involves the spontaneous release of the hemin from the heme pocket.

The preference in the initial heme orientation noted upon selective removal of propionate side chains, however, suggests that the failure to detect the likely initially rotationally disordered protoporphyrin results from rapid equilibration. The absence of the F8-His–iron bond in the desFe Mb is likely to increase significantly the rate of spontaneous heme release because of the elimination of the need to break the very stable His–iron bond.[5,8]

In the absence of specific interaction between the heme pocket and the organic co-solvent needed to solubilize the prosthetic group during the reconstitution (*i.e.*, the case of DMSO), the initial preferences for the two alternate heme orientations for 6-methyl-6-despropionate-hemin (as in B of Figure 1, with R_6 = CH_3, R_7 = propionate) and 7-methyl-7-despropionate-hemin (as in A of Figure 1, with R_6 = propionate, R_7 = CH_3) are very strong. The small (~20%) amount of orientation for the former hemin detected after removal of DMSO may have resulted from equilibration on the column.

When pyridine is used as the co-solvent, both 6-methyl-6-despropionate-hemin and 7-methyl-7-despropionate-hemin lose some, but definitely not all, of their strong preference for the initial heme orientation. Since the pyridine (but not the DMSO) also induces large spectral changes for metMbCN, the loss of preference suggests that the pyridine interacts with the hemin in the intact pocket, and the interaction itself modulates the nature of the initial complex. Thus if an organic co-solvent is essential for solubility reasons, DMSO is preferable to pyridine.

Interaction of metMbCN with Pyridine. The observation only of peaks with intermediate shift and line width between that of pure metMbCN and that with 2.5 mol % pyridine-$^2H_5$, at which point the spectral parameters become independent of the pyridine $^2H_5$:^2H_2O ratio, dictates that we are observing completely averaged spectra, with the interconversion rate between contributing species much greater than the maximum shift differential[26] (rate > ~10^4 s^{-1}). The binding constant for the fit to the data in Figure 6 is consistent with, but not proof of, a 1:1 complex formation.

The fact that a completely different ^1H NMR spectrum is obtained when pyridine-$^2H_5$ is added to metMbH$_2$O in the absence of cyanide (Figure 5D) argues that the pyridine is interacting with the intact metMbCN complex and does not displace the bound cyanide. The possibility that the pyridine displaces the bound proximal His F8 can also be eliminated, since the strongly shifted peaks for the axial imidazole side chain,[27] b and y in Figure 5A, experience even larger hyperfine shifts and retain their characteristic large line width due to their proximity to the iron.

A clue to the nature of the binding site of the pyridine in the heme pocket of metMbCN is obtained by considering the spatial selectivity of the induced shifts. Inspection of the spectra in parts A and B of Figure 5, as well as the data in Figure 6 and Table III, reveals that, for the resolved peaks, addition of pyridine influences primarily the shifts for the heme[4,28,29] (a = 5-CH_3, c = 1-CH_3, d = 2-H_α, f = 8-CH_3, v = 2-$H_{\beta t}$) and the amino acid resonances His 93 F8 peaks b, y (ring δ-H, ϵ-H),[27] and i (β-CH),[28,29,30,31] and Ile 99 FG5 peaks[32] w, x, z (δ-CH_3, γ-CH_3, γ-CH), but inconsequentially those of Phe 43 CD1 peaks[25] e (p-H), g (m-H), His 64 E7 peak[30] h (ring ϵ-H), or Val 68 E11 peak[31] v (α-CH).

The residues His F8 and Ile FG5 are on the proximal side of the heme, while His E7, Val E11, and Phe CD1 are on the distal side.[9] The much larger perturbations of the proximal side residues compared to the three distal side residues suggest that the pyridine intercalates on the proximal side of the heme rather than in the distal heme cavity. The major perturbation of His F8 suggests a plausible binding site for the pyridine is the "Xenon" hole, a hydrophobic vacancy above pyrrole I which makes contact with His F8. In addition to binding Xenon[33,34] the cavity is known to accommodate a variety of organic[35] (cyclopropane) or inorganic[36,37] (AuI_3, $H_3I_3^-$) species. The strongest perturbation of heme resonances is for the 8-CH_3, with the next largest effect on 1-CH_3 and 2-vinyl peaks. This is similar to the pattern of perturbations observed[28] when Xenon or cyclopropane intercalates within the hydrophobic vacancy over pyrrole I in metMbCN. Competition experiments with cyclopropane and pyridine were inconclusive, probably because, like with Xenon,[34] there are multiple binding sites within the protein that interact with each other. The fact that addition of DMSO causes no detectable change in either shift or line width argues that it does not have similar access to the heme cavity. The possibility exists that pyridine interacts in a similar manner with apoMb which is proposed to have a similar, although much less rigid, structure[18] than holoMb. It is noted that reconstituting apoMb with native hemin does not influence

(25) Emerson, S. D.; Lecomte, J. T. J.; La Mar, G. N. *J. Am. Chem. Soc.* **1988**, *110*, 4176–4182.

(26) Sandström, J. *Dynamic NMR Spectroscopy*; Academic Press: New York, 1981; Chapter 2.

(27) La Mar, G. N.; de Ropp, J. S.; Chacko, V. P.; Satterlee, J. D.; Erman, J. E. *Biochim. Biophys. Acta* **1982**, *708*, 317–325.

(28) Mayer, A.; Ogawa, S.; Shulman, R. G.; Yamane, T.; Cavaleiro, J. A. S.; Rocha-Gonsalver, A. M. d'A.; Kenner, G. W.; Smith, K. M. *J. Mol. Biol.* **1974**, *86*, 887–896.

(29) Ramaprasad, S.; Johnson, R. D.; La Mar, G. N. *J. Am Chem. Soc.* **1984**, *106*, 3632–3635.

(30) Lecomte, J. T. J.; La Mar, G. N. *Eur. Biophys. J.* **1986**, *13*, 373–381.

(31) Emerson, S. D. Ph.D. Dissertation, University of California, Davis, 1988.

(32) Ramaprasad, S.; Johnson, R. D.; La Mar, G. N. *J. Am. Chem. Soc.* **1984**, *106*, 5330–5335.

(33) Bluhm, M. M.; Bodo, G.; Dintzis, H. M.; Kendrew, J. C. *Proc. R. Soc.* **1958**, *A246*, 369–389.

(34) Tilton, R. F., Jr.; Kuntz, J. D., Jr.; Petsko, G. A. *Biochemistry* **1984**, *23*, 2849–2852.

(35) Schoenborn, B. P.; Watson, H. C.; Kendrew, J. C. *Nature* **1965**, *207*, 28–30.

(36) Schoenborn, B. P. *Nature* **1967**, *214*, 1120–1122.

(37) Kretsinger, R. H.; Watson, H. C.; Kendrew, J. C. *J. Mol. Biol.* **1968**, *31*, 305–314.

the 1:1 ratio of the two heme orientations formed during the initial contact (Figure 5E). However, it appears to act to diminish some of the strong preference in the heme orientation for the metal complex for the initial propionate contact for 6-methyl-6-despropionate-hemin (compare trace B and A of Figure 3) and 7-methyl-7-despropionate-hemin (compare traces B and A of Figure 4).

Structure of desFe Mb. The typical upfield ring-current shifted Val E11 γ-CH_3 peak in desFe Mb[19] confirms a heme pocket structure similar to that of MbCO.[24] However, both the upfield Val CH_3 and low-field meso-H ring current shifts are significantly larger than in MbCO[24] (compare in Table I). In fact, the low-field meso-H shifts are larger in desFe Mb than either MbCO[24] model complexes or free protoporphyrins,[38,39] which exhibit mean meso-H shifts ~9.8 ppm. The mean meso-H shift (10.3 ppm) in desFe Mb, however, is in the direction of that recorded for protoporphyrin IX in trifluoroacetic acid,[40] in which it exists as a dication, with mean meso-H shift ~11.0 ppm. Such dication formation has been shown to lead to substantial increase in the ring current due to resonance stabilization.[39-41] The ~40% of the low-field bias toward the dication suggests an intermediate state of protonation. Thus both the low-field bias of meso-H and upfield bias of Val E11 CH_3 in desFe Mb relative to MbCO strongly suggests protonation of the prosthetic group. While such an effect may not be expected in a presumed relatively nonpolar heme pocket, it could arise from strong hydrogen bonding between the protonated imidazolium side chains of the proximal His F8 and a porphyrin ring imine nitrogen. The structure of the complex is under further study.

(38) Caughey, W. S.; Barlow, C. H.; O'Keeffe, D. H.; O'Toole, M. C. *Ann. NY Acad. Sci.* **1973**, *200*, 296-308.
(39) Janson, T. R.; Katz, S. S. *The Porphyrins* **1978**, *4B*, 1-59.
(40) Abraham, R. J.; Jackson, A. H.; Kenner, G. W. *J. Chem. Soc.* **1961**, *3*, 3468-3474.
(41) Abraham, R. *J. Mol. Phys.* **1961**, *4*, 145-152.

Conclusions

The formation of holo-Mb with a 1:1 mixture of hemin rotationally disordered about the α,γ-meso axis in the initial complex formed during the reconstitution of Mb is due to the formation of a relatively stable salt bridge between a single propionate group and a unique protein residue, possibly Arg CD3. Removal of one of the propionate groups leads to a strong preference for one of the orientations that places the sole propionate into the position occupied by the 6-propionate group in the Mb X-ray structure. The pyridine solvent used to solubilize the hemin for reconstitution was found to interact specifically with the protein complex on the proximal side of the heme.

Acknowledgment. The authors are indebted for experimental assistance to the staff of the UCD NMR Facility. This research was supported by grants from the National Institutes of Health (HL-16087 and HL-22252).

NMR Distance Constraint Analysis for the Aglycon of Aridicin A Bound to Ac-Lys(Ac)-D-Ala-D-Ala. A New Method for Predicting Well-Defined and Variable Regions of Molecular Conformation Defined by Distance Constraints

Judith C. Hempel

Contribution from the Department of Physical and Structural Chemistry, Smith Kline and French Laboratories, Swedeland, Pennsylvania 19479. *Received May 2, 1988*

Abstract: Over 100 NMR-derived distance constraints are reported in a companion paper[1] for the aglycon of Aridicin A bound to the tripeptide Ac-Lys(Ac)-D-Ala-D-Ala. Even though the distance constraints are not as precisely determined as chemical bonds, correlated NOEs severely constrain the conformation of clusters of structural templates of the molecular complex. Overlapping clusters extend the regions of restricted conformation. A methodology is introduced to map the clusters of structural templates defined by the data set. The map reveals the regions of the molecular complex where the conformation is defined and regions where it is not. The more highly correlated the distance constraints, the more restricted the conformation of the molecular domain. The relevance of this ab initio analysis of the distance constraints is demonstrated with an analysis of seven molecular models for the solution conformation of the molecular complex generated by distance geometry. Conformational domains predicted by the ab initio analysis are observed in the molecular modeling study.

Aridicin A is a member of the vancomycin/ristocetin class of glycopeptide antibiotics. The aglycon of Aridicin A is a heptapeptide in which the aromatic side chains of residues 1 and 3 are linked, as are the side chains of residues 2 and 4, 4 and 6, and 5 and 7 (see Figure 1). The seven residues are named GCFBEAD proceeding from the N to the C terminus of the peptide in agreement with a previously defined convention.[2] The action of this class of antibiotics is postulated to involve binding to D-alanyl-D-alanine residues at the C terminus of bacterial cell wall components.[3] NMR studies are reported in a companion paper[1] for complexes of the aglycon of Aridicin A bound to the bacterial cell wall fragments Ac-Lys(Ac)-D-Ala-D-Ala and Ac-Ala-γ-D-Gln-Lys(Ac)-D-Ala-D-Ala. NMR-derived distance constraints are the same for the region common to both complexes. A single solution conformation model that satisfies all NMR-derived distance constraints for the molecular complex with tripeptide has been proposed.[1]

(1) Mueller, L.; Heald, S. L.; Hempel, J. C.; Jeffs, P. W. *J. Am. Chem. Soc.*, following paper in this issue.
(2) Jeffs, P. W.; Mueller, L.; DeBrosse, C.; Heald, S. L.; Fisher, R. *J. Am. Chem. Soc.* **1986**, *108*, 3063-3075.
(3) (a) Reynolds, P. E. *Biochim. Biophys. Acta* **1961**, *52*, 403-405. (b) Jordan, D. C. *Biochim. Biophys. Res. Commun.* **1961**, *6*, 16-170. (c) Perkins, H. R. *Biochem. J.* **1969**, *111*, 195-205.

0002-7863/89/1511-0491$01.50/0